1. Sami Mohammed BENNIHI[1], 2. Seddik TOUHAMI[2], 3. Wessim AKSA[3]

IRECOM Laboratory, Department of Electrical Engineering, Djillali Liabes University, Sidi Bel Abbes, Algeria (1,2,3)
ORCID: 1. 0000-0002-6134-5825

doi:10.15199/48.2023.12.03

Modeling of the Electrostatic Separation Process in a Novel Turntable Installation for the Plastic Waste Recycling Process

Abstract. *This paper investigates particle electrostatic separation inside a new conical rotary installation using the discrete element method to understand particle behavior related to multiple variables such as the applied high-voltage, particle charge, and mass. The model offers the ability to monitor and control all significant parameters at particle level. The results have been analyzed using the response surface methodology to further understand the relationships between variables. These findings could serve as a blueprint for the manufacturing of an efficient industrial device.*

Streszczenie. *Artykuł ten bada separację elektrostatyczną cząstek wewnątrz nowej stożkowej instalacji obrotowej przy użyciu metody elementów dyskretnych, aby zrozumieć zachowanie cząstek związane z wieloma zmiennymi, takimi jak przyłożone wysokie napięcie, ładunek cząstek i masa. Model oferuje możliwość monitorowania i kontrolowania wszystkich istotnych parametrów na poziomie cząstek. Wyniki zostały przeanalizowane przy użyciu metodologii powierzchni odpowiedzi, aby lepiej zrozumieć zależności między zmiennymi. Odkrycia te mogą posłużyć jako plan produkcji wydajnego urządzenia przemysłowego (**Modelowanie procesu separacji elektrostatycznej w nowatorskiej instalacji ze stołem obrotowym do procesu recyklingu odpadów z tworzyw sztucznych**)*

Keywords: Discrete element method, Granular flow, Response surface methodology, Numerical model
Słowa kluczowe: Metoda elementów dyskretnych, przepływ granularny, metodologia powierzchni odpowiedzi, model numeryczny

Introduction

To The past decades have seen a revolution within the recycling industry, with advanced and efficient processes that rely on the environmentally friendly electrostatic separation method [1-3]. Not only environmental and material consumption growth problems are highlighted [4], but also the rise in oil and gas prices in the past few years worldwide for political reasons is pushing the need for investments in technologies that can preserve resources from that ilk [5-7]. In an attempt to handle granular plastic wastes generated from electric and electronic equipment (WEEE), which can remain undecomposed for decades, avoiding landfilling, burning, or acid washing [8].

The basic notion of electrostatic separation is the deliberate categorization of charged or polarized materials inside an electric field [9-10]. For an effective selection, materials are pulverized into small granular particles and charged by ion bombardment, induction, or contact electrification, then introduced to the electric field responsible for the attraction or repulsion of particles depending on their charge (positive or negative) [11-15].

On one hand, the random shape and nature of the granular materials impose more often than not restraints related to the contact between particles or walls, cohesion, coulombic effect, gravitational force, and so on, which are difficult to prevail over. On the other hand, most classical installations require considerable space, which is not optimal in a crowded environment. Moreover, the middling products and their need for further processing, which decays the separation quality, pose more problems on an industrial scale [16-19].

If an industrial installation is to be manufactured, an in-depth study must be conducted to foresee and estimate the potential, characteristics, and dimensions of any new design. Mathematical models can help reduce the time required and narrow down the number of prototypes needed for an industrial build. In an effort to enhance the effectiveness of electrostatic separation, this study presents a modern methodology combining the Discrete Element Method (DEM) and Response Surface Methodology (RSM) simulations to maximize the efficiency of the process.

DEM proved to be a very accurate and efficient method for predicting discrete particulate behavior in environments where data acquisition can be difficult or impossible across several industries, such as powder, mining, pharmaceutical, chemical, food, recycling, and mineral industries. While RSM was utilized to analyze and optimize the separation process by finding the relationship and impact of the different variables to identify the input variable combination that maximizes the separation efficiency (response) [20-22].

The new unconventional installation shown in Figure 1 was built using two parallel conical electrodes (radi = 120 mm; $\Theta = 20^{o}$); the lower (earthed) electrode is linked to the upper electrode (connected to a DC source) via adjustable bars that allow controlling the inter-electrode distance. The gap in the upper electrode serves as an insertion point for the materials to be sorted. The assembly is deposited on a vertical motor responsible for the rotation of the coupled cones [23-24].

The blend intended for separation is introduced at a given speed and travels through an electric field generated between the two electrodes. The positively charged particles slide for a brief moment on the surface of the lower electrode, then get elevated and thrown towards the outer collector cell with the help of the electrostatic and centrifugal forces that also prevent particles from sticking to the surface of the electrodes, while the negatively charged particles slide downwards to the inner collector cell directly.

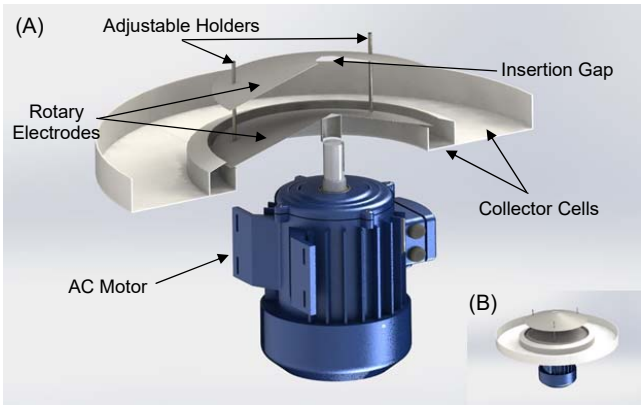

Fig.1. Representation of the conical rotary electrostatic separator with a cross-section view (A) and full view (B)

Methodology

The computations were performed with the help of the reputed open-source software LIGGGHTS 3.8.0 mainly using a range of millimetric plastic granular particles in a closed simulation domain containing the geometry as well. By integrating Newton's second law of motion, the total forces exerted on each particle were computed, which gave the particle positions and trajectories. The general translational and rolling motion [25-28] of particles were computed as follows:

(1) $$m.a = \sum F$$

(2) $$I\frac{d\omega}{dt} = \sum \tau$$

Where m, a, F, I, ω, τ are particle mass, acceleration, total force, inertia, angular velocity and total torque. The main forces involved in particle motion are the gravitational force Fg, the electrostatic force Fel, contact force Ff and centrifugal force Fc mathematically expressed as:

(3) $$F_g = m.g$$

(4) $$F_{el} = q.E$$

(5) $$F_f = F_n + F_t$$

(6) $$F_c = m\frac{v^2}{R}$$

Where g, q, E, v, R, Fn, Ft are gravitational constant, particle charge, electric field, velocity, radius, normal and tangential components of the contact force. The external electric field [29] is proportional to the inter-electrodes distance d, and the high-voltage applied V can be given as:

(7) $$V = d.E$$

The sample used is a blend of spherical particles composed of 50% ABS and 50% PE typically from WEEE with masses ranging from 10-28 mg. A total of 27 runs have been performed to evaluate the three distinguished factors: the high voltage applied, particle charge, and inter-electrode distance deemed most relevant for an optimum electrostatic separation procedure. The speed of the electrodes was kept constant at 60 RPM during the simulations. The post-processing of particle positioning and visualization was done using ParaView 5.10.1 to optimize the results [30].

The particle properties and characteristics used for the DEM simulations are summarized in Table 1. The contact model employed for this study was the Hertz and Mindling model without cohesion. The time-step size was under 10% of the Rayleigh and Hertz critical time steps [31-36]. Additional simulations were performed to assess the effect of the deformation parameters, which did not affect the separation aspect considerably

Table 1. Simulation material properties of particles

Properties	Value
Young's modulus [Pa]	5.e6
Poisson's ratio [-]	0.35
Coefficient of restitution [-]	0.45
Coefficient of static friction [-]	0.4
Coefficient of rolling friction [-]	0.01
Particle density [kg/m3]	1250
Mass [mg]	10-28
Radius [mm]	1.25-1.75
Mass rate [kg/s]	0,014
Constant insertion velocity [m/s]	0.5

RSM was employed to analyze the relation between the response (recovery of the collected product) and the multiple independent factors investigated [37-40] in this study by DEM considered most influential for the electrostatic separation process. Table 2 summarizes the factors evaluated using RSM and their variation domains. Since there was no prior information regarding the relationship between the response and the factors mentioned above, the model can be represented by the second-order nonlinear quadratic polynomial [41-43] as follows:

(8) $$Y = A_0 + \sum_{i=1}^{k} A_i Z_i + \sum_{i=1}^{k} A_{ii} Z_i^2 + \sum_i \sum_j A_{ij} Z_i Z_j + \varepsilon$$

Where Y, k, ε, A0, Ai, Aii, Aij are the predicted response, number of variables, random error, constant, the coefficients of linear, quadric, and interaction parameters, respectively. For the three variables used [44-45] in the second-order generalized model RSM response becomes:

(9) $$Y = A_0 + \sum_{i=1}^{k} A_i Z_i + \sum_{i=1}^{k} A_{ii} Z_i^2 + \sum_i \sum_j A_{ij} Z_i Z_j + \varepsilon$$

Table 2. Factors and variation domain

Factor	Min	Max
U	20	60
Q	0.1	0.5
d	5	15

Table 3. DEM Electrostatic separation results

Run	U [kV]	Q [nC]	d [cm]	Rec ABS [%]
1	20	0,4	5	18,74
2	30	0,4	5	68,05
3	40	0,4	5	94,74
4	50	0,4	5	100
5	60	0,4	5	100
6	20	0,4	10	0,22
7	30	0,4	10	4,83
8	40	0,4	10	17,09
9	50	0,4	10	32,51
10	60	0,4	10	60,33
11	20	0,4	15	0,1
12	30	0,4	15	0,22
13	40	0,4	15	3,67
14	50	0,4	15	8,16
15	60	0,4	15	16,81
16	40	0,1	5	0,32
17	40	0,2	5	35,55
18	40	0,3	5	81,11
19	40	0,5	5	97,04
20	40	0,1	10	0
21	40	0,2	10	0,32
22	40	0,3	10	8,25
23	40	0,5	10	18,91
24	40	0,1	15	0
25	40	0,2	15	0
26	40	0,3	15	0,22
27	40	0,5	15	5,76

The variables from Table 3 were used to calculate the coefficients of quadratic equation and the ABS recovery results (Rec_{ABS}) from DEM computations used as responses.

Results and discussion

The final positions of ABS (red) and PE (blue) particles distinguished by their charges inside the collector cells after

the electrostatic separation process are displayed in Figure 2 in the simulation environment. The best results were obtained with the shortest inter-electrode distance (d = 5 cm) with up to 95% recovery for U = 40 kV. However, poor recovery results were noted for the other cases, especially for d = 15 cm shown in (c) and (f), respectively, which is not recommended for medium or large particles due to the electrostatic force being divided by three and therefore the gravitational force dominating the process. The outer box had only ABS particles, which suggests that the coulomb force was not significant for the sample used, as a consequence the purity remained immaculate.

The collected mass of the binary mixture of ABS and PE products as a function of the applied high-voltage Figure 3 and particle charge Figure 4 respectively, summarizes the impact of both variables for the three inter-electrode distances on the electrostatic separation. A drastic increase of 77 % in ABS mass collection at U = 40 kV between d = 5 and 10 cm occurred. Likewise, the mass difference for Q = 0,3 between d = 5 and 10 cm went up by 73%, which highlights the impact of the electrostatic force and the electrode distance.

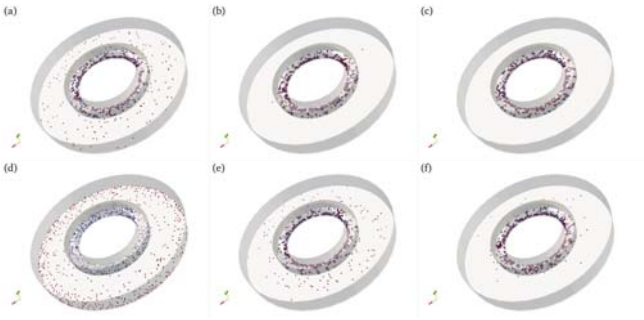

Fig.2. Snapshots of particle distribution in the collector cell for U = 20 kV; Q = 0,4 nC and d = 5, 10, and 15 cm in (a), (b), and (c), respectively; and for U = 40 kV; Q = 0,4 nC and d = 5, 10, and 15 cm in (d), (e), and (f), respectively

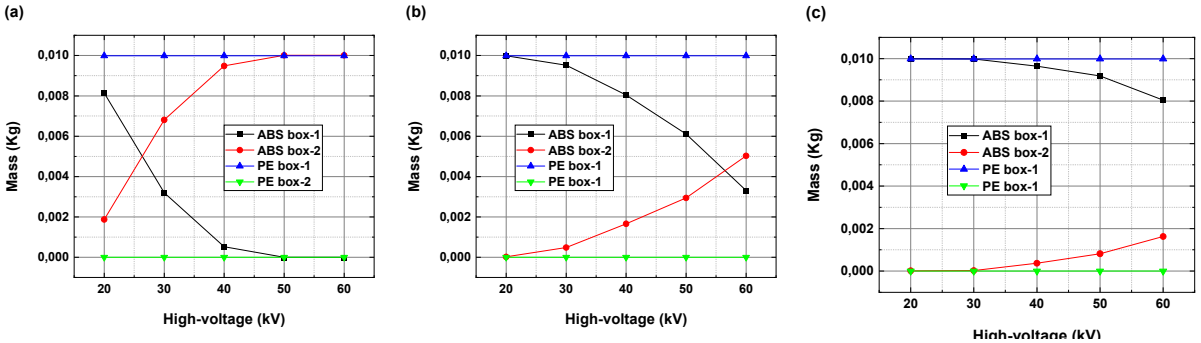

Fig.3. Variation of the collected mass of ABS and PE in the collectors for a constant charge Q = 0,4 nC and inter-electrode distance d = 5, 10, and 15 cm in (a), (b), and (c) respectively vs high-voltage (U)

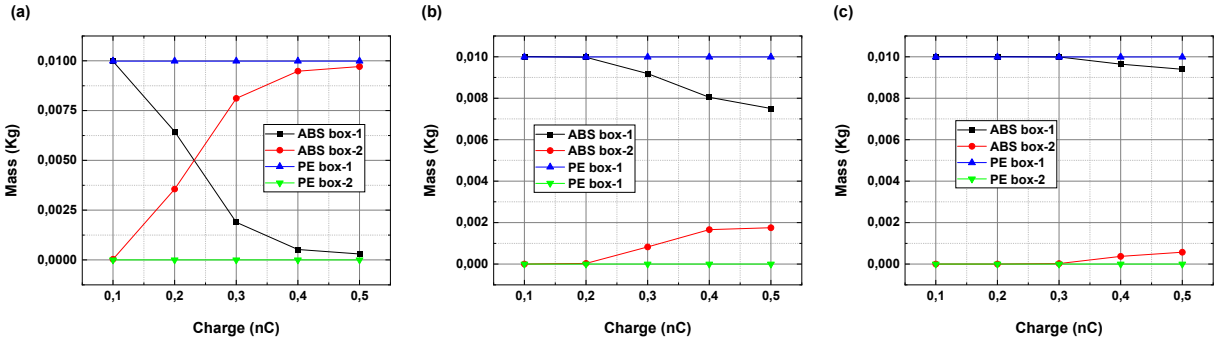

Fig.4. Variation of the collected mass of ABS and PE in the collectors for a constant high-voltage U = 40 kV and inter-electrode distance d = 5, 10, and 15 cm in (a), (b), and (c) respectively vs the charge (Q)

The Pareto chart in Figure 6 serves to define the relevance and magnitude of each term on the response [46-47]. The bars display the values of the impacts from highest to lowest. The red line at 2.09 is used as a reference to identify the statistically significant factors; in this study, only the relevant factors that exceeded the reference line are kept, and the most influential factor would be factor B, which represents the inter-electrode distance, which should be prioritized to optimize the results, then the high-voltage and the charge come afterwards.

Regression RMS response equation for Rec_{ABS} by eliminating the insignificant terms as a function of variables is given by:

$$Rec_{ABS} = -64,4 + 2,810\,U - 8,42\,d + 310,4\,Q + 0,768\,d^2 - 0,1531\,U \times d - 20,44\,d \times Q \quad (10)$$

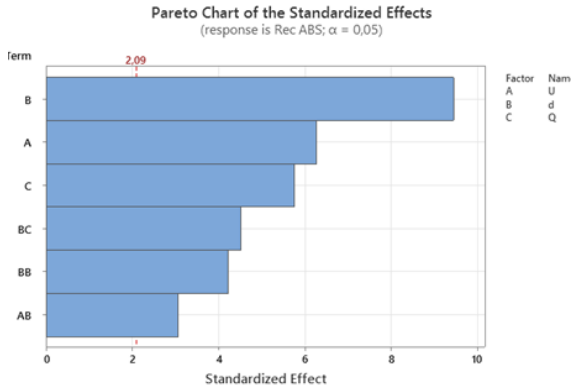

Fig.5. Pareto chart for significant variables

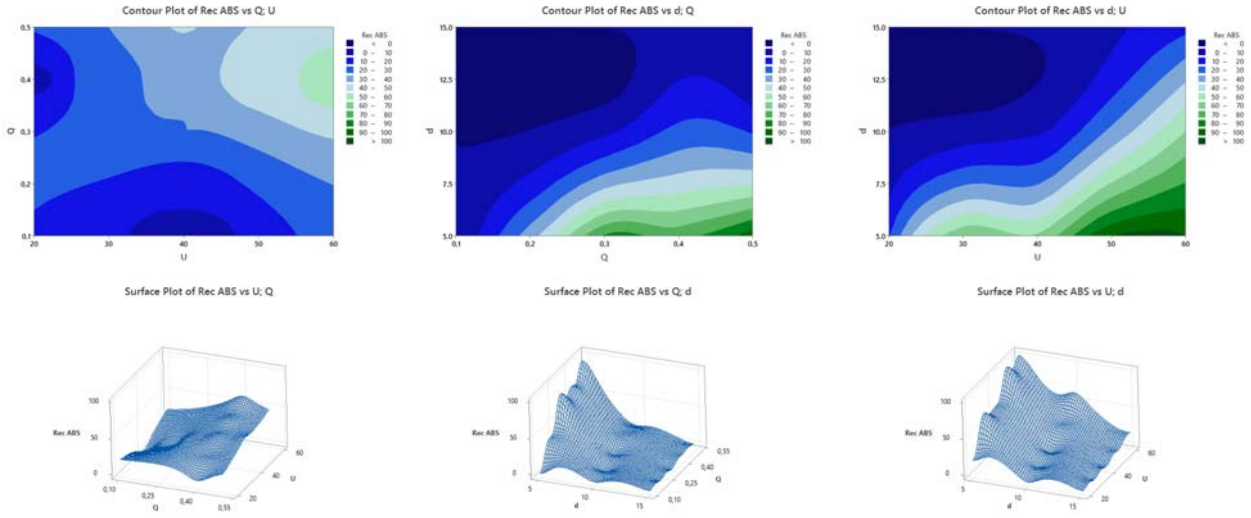

Fig.6. Contour plots (a, b, c) and surface plots (d, e, f) for ABS particle recovery using different independent variables

RSM contour plots (2D) and surface plots (3D) shown in Figure 5 provide a graphical illustration of the regions of interactions amongst the different variables and their impact on ABS particle recovery in the outer collector. They allow the monitoring of changes in the response if one or more input variables vary. Visually examining the plots gives insights into the nature and importance of these associations. These relationships help pinpoint the combination of variables that yields the desired response.

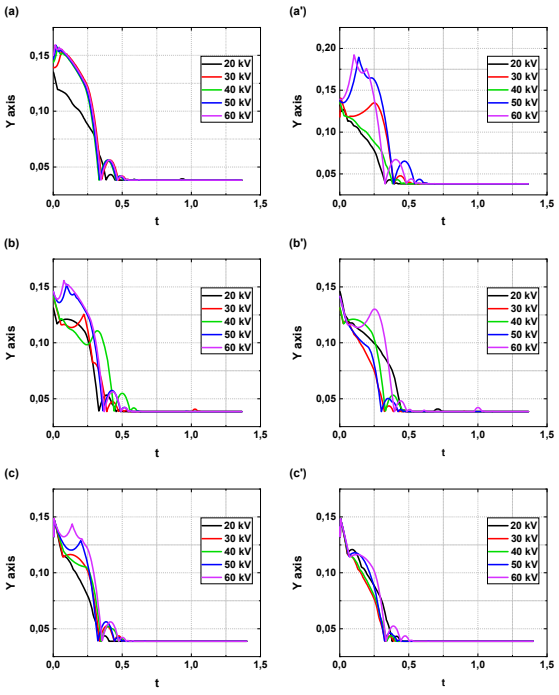

Fig.7. Particle trajectories on the Y axis vs. time for m = 10 mg (a), (a'); 17 mg (b), (b'); 28 mg (c), (c'), respectively, for different high-voltage values

The Individual particle trajectories on the Oy axis for d = 5 and 10 cm have been computed to analyze the particle take-off based on the particle sizes used. As predicted, the results indicate that the variation of the electrostatic field intensity Figure 7 and particle charge Figure 8 had a direct correlation with particle lifting dynamics. Several characteristics play a role in particle height and suspension time. Larger or heavier particles have slower ascension time and height compared to smaller or lighter particles due to gravity, size, mass, insertion velocity.

For d = 5 cm a high-voltage of 30 kV and charge of 0,2 nC were enough for small-sized particles rapid take-off, but higher voltage and charge values are needed to lift medium-sized and large-sized particles. When it comes to d = 10 cm, at least 50 kV and 0,4 nC are needed for small-sized particles, whereas no taking-off took place for the rest of the particles, indicating the dominance of gravitational forces. The outcomes for d = 15 cm were unsatisfactory, with no significant lift-off taking place using the same conditions, and therefore ignored.

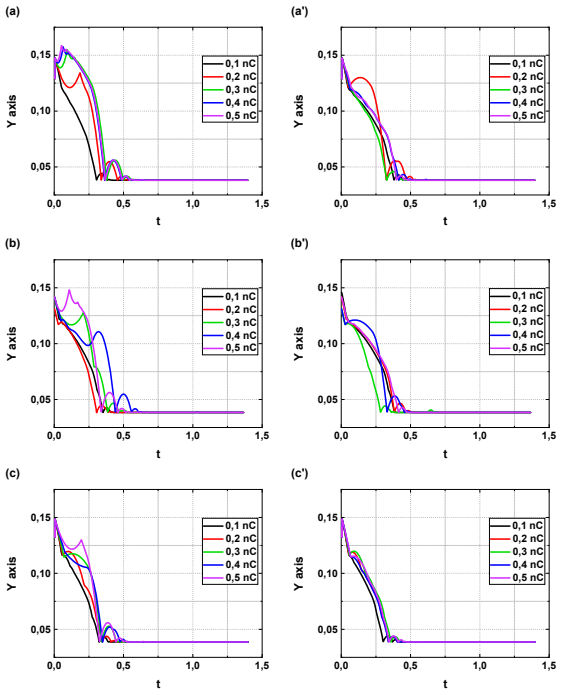

Fig.8. Particle trajectories on the Y axis vs. time for m = 10 mg (a), (a'); 17 mg (b), (b'); 28 mg (c), (c'), respectively, for different particle charge values

Conclusions

The novel installation for the electrostatic separation of granular particles has been modeled and analyzed in this paper. The working conditions and the feasibility of the process have been studied using DEM simulations and analyzed using RSM. Within the simulation domain, the recovered particle mass relies heavily on the electric field intensity, particle charge, and inter-electrode distance. The simulations show the role of the gravitational force that dominates the process for large particles and show that increasing the high-voltage or electric charge does not necessarily lead to better separation results. These findings underscore the importance of considering particle size when studying particle take-off phenomena. Overall, the varying results from simulations gave emphasis to the influence of different parameters or factors on the electrostatic separation. It is worth mentioning that different factors could impact the outcomes, such as the presence of an aerodynamic or cohesive force; also, particle agglomeration could have an impact, which needs further investigation. Nevertheless, the outcomes of this study provide valuable insights that could help in the manufacturing and optimization of a future industrial installation.

Acknowledgments

This work was supported by Interaction Réseaux Electriques Convertisseurs Machines (IRECOM) Laboratory University Djillali Liabes, Sidi Bel Abbès, 22000, Algeria. The authors would like to offer a special thanks to Thomas Leps for his expertise and guidance in the development of the DEM model.

***Authors**:*

PhD. student Sami Mohammed Bennihi, Department of Electrical Engineering, IRECOM Laboratory, Faculty of Electrical Engineering, University of Djillali Liabes, Sidi Bel Abbes, Algeria, Email: bennihi.sami@gmail.com; sami.bennihi@univ-sba.dz;

Dr. Seddik Touhami, Department of Electrical Engineering, IRECOM Laboratory, Faculty of Electrical Engineering, University of Djillali Liabes, Sidi Bel Abbes, Algeria,
E-mail: seddik.touhami@gmail.com;

Professor. Wessim Aksa, Department of Electrical Engineering, IRECOM Laboratory, Faculty of Electrical Engineering, University of Djillali Liabes, Sidi Bel Abbes, Algeria,
E-mail: aksa86wessim@gmail.com

REFERENCES

[1] A. Catinean, L. Dascalescu, M. Lungu, L. M. Dumitran, and A. Samuila, "Improving the recovery of copper from electric cable waste derived from automotive industry by corona-electrostatic separation," *Particulate Science and Technology*, vol. 39, no. 4, pp. 449–456, May 2021, doi: 10.1080/02726351.2020.1756545.

[2] P. R. Dias *et al.*, "High yield, low cost, environmentally friendly process to recycle silicon solar panels: Technical, economic and environmental feasibility assessment," *Renewable and Sustainable Energy Reviews*, vol. 169, p. 112900, Nov. 2022, doi: 10.1016/j.rser.2022.112900.

[3] E. O. Opare, E. Struhs, and A. Mirkouei, "A comparative state-of-technology review and future directions for rare earth element separation," *Renewable and Sustainable Energy Reviews*, vol. 143, p. 110917, Jun. 2021, doi: 10.1016/j.rser.2021.110917.

[4] E. G. Shershneva, "Plastic Waste: Global Impact and Ways to Reduce Environmental Harm," *IOP Conf. Ser.: Mater. Sci. Eng.*, vol. 1079, no. 6, p. 062047, Mar. 2021, doi: 10.1088/1757-899X/1079/6/062047.

[5] M. A Kassem, M. A. Khoiry, and N. Hamzah, "Theoretical review on critical risk factors in oil and gas construction projects in Yemen," *ECAM*, vol. 28, no. 4, pp. 934–968, Apr. 2021, doi: 10.1108/ECAM-03-2019-0123.

[6] J. D. Colgan, "Oil, Domestic Politics, and International Conflict," *Energy Research & Social Science*, vol. 1, pp. 198–205, Mar. 2014, doi: 10.1016/j.erss.2014.03.005.

[7] N. Sakib, N. U. Ibne Hossain, F. Nur, S. Talluri, R. Jaradat, and J. M. Lawrence, "An assessment of probabilistic disaster in the oil and gas supply chain leveraging Bayesian belief network," *International Journal of Production Economics*, vol. 235, p. 108107, May 2021, doi: 10.1016/j.ijpe.2021.108107.

[8] M. Gliniak, "The possibilities of automation of the manual line for dismantling waste electrical and electronic equipment," *Przeglad Elektrotechniczny*, vol. 1, no. 6, pp. 138–141, Jun. 2018, doi: 10.15199/48.2018.06.26.

[9] A. V. M. Silveira, M. Cella, E. H. Tanabe, and D. A. Bertuol, "Application of tribo-electrostatic separation in the recycling of plastic wastes," *Process Safety and Environmental Protection*, vol. 114, pp. 219–228, Feb. 2018, doi: 10.1016/j.psep.2017.12.019.

[10] J. Li and Z. Xu, "Compound tribo-electrostatic separation for recycling mixed plastic waste," *Journal of Hazardous Materials*, vol. 367, pp. 43–49, Apr. 2019, doi: 10.1016/j.jhazmat.2018.12.017.

[11] L. Dascalescu, T. Zeghloul, and A. Iuga, "Electrostatic Separation of Metals and Plastics From Waste Electrical and Electronic Equipment," in *WEEE Recycling*, Elsevier, 2016, pp. 75–106. doi: 10.1016/B978-0-12-803363-0.00004-3.

[12] K. Dong, Q. Zhang, Z. Huang, Z. Liao, J. Wang, and Y. Yang, "Experimental Investigation of Electrostatic Reduction in a Gas–Solid Fluidized Bed by an in Situ Corona Charge Eliminator," *Ind. Eng. Chem. Res.*, vol. 53, no. 37, pp. 14217–14224, Sep. 2014, doi: 10.1021/ie501584v.

[13] G. S. P. Castle, "A Century of Development in Applied Electrostatics [History]," *IEEE Ind. Appl. Mag.*, vol. 16, no. 4, pp. 8–13, Jul. 2010, doi: 10.1109/MIAS.2010.937301.

[14] W. Wei and Z. Gu, "Electrification of particulate entrained fluid flows—Mechanisms, applications, and numerical methodology," *Physics Reports*, vol. 600, pp. 1–53, Oct. 2015, doi: 10.1016/j.physrep.2015.10.001.

[15] F. Mach, P. Kus, P. Karban, and I. Dolezel, "Higher-Order Modeling of Electrostatic Separator of Plastic Particles," *Przeglad Elektrotechniczny*, vol. 88, pp. 74–76, Jan. 2012.

[16] J. Li, Q. Zhou, and Z. Xu, "Real-time monitoring system for improving corona electrostatic separation in the process of recovering waste printed circuit boards," *Waste Manag Res*, vol. 32, no. 12, pp. 1227–1234, Dec. 2014, doi: 10.1177/0734242X14554647.

[17] K. Enders, A. S. Tagg, and M. Labrenz, "Evaluation of Electrostatic Separation of Microplastics From Mineral-Rich Environmental Samples," *Front. Environ. Sci.*, vol. 8, p. 112, Jul. 2020, doi: 10.3389/fenvs.2020.00112.

[18] J. Li and L. Dascalescu, "Newly-Patented Technical Solutions for improving the Tribo-Electrostatic Separation of Mixed Granular Solids," *ENG*, vol. 6, no. 2, pp. 104–115, Jun. 2012, doi: 10.2174/187221212801227158.

[19] W. Jiang, L. Jia, and X. Zhen-ming, "A new two-roll electrostatic separator for recycling of metals and nonmetals from waste printed circuit board," *Journal of Hazardous Materials*, vol. 161, no. 1, pp. 257–262, Jan. 2009, doi: 10.1016/j.jhazmat.2008.03.088.

[20] A. Phillip Grima and P. Wilhelm Wypych, "Discrete element simulations of granular pile formation: Method for calibrating discrete element models," *Engineering Computations*, vol. 28, no. 3, pp. 314–339, Apr. 2011, doi: 10.1108/02644401111118169.

[21] D. Sun, L. Zhao, G. Liang, and H. Zhou, "Prediction of Bolted Joint Dynamics Based on the Thin-Layer Element of Nonlinear Material," *ACSM*, vol. 43, no. 5, pp. 311–315, Nov. 2019, doi: 10.18280/acsm.430506.

[22] Yeom, Ha, Kim, Jeong, Hwang, and Choi, "Application of the Discrete Element Method for Manufacturing Process Simulation in the Pharmaceutical Industry," *Pharmaceutics*, vol. 11, no. 8, p. 414, Aug. 2019, doi: 10.3390/pharmaceutics11080414.

[23] D. J. Choszcz, P. S. Reszczyński, E. Kolankowska, S. Konopka, and A. Lipiński, "The Effect of Selected Factors on Separation Efficiency in a Pneumatic Conical Separator," *Sustainability*, vol. 12, no. 7, p. 3051, Apr. 2020, doi: 10.3390/su12073051.

[24] M. Berggren, R. Zubrin, P. Jonscher, and J. Kilgore, “Lunar Soil Particle Separator,” in *49th AIAA Aerospace Sciences Meeting including the New Horizons Forum and Aerospace Exposition*, Orlando, Florida: American Institute of Aeronautics and Astronautics, Jan. 2011. doi: 10.2514/6.2011-436.

[25] C. Kloss, C. Goniva, A. Hager, S. Amberger, and S. Pirker, “Models, algorithms and validation for opensource DEM and CFD-DEM,” *PCFD*, vol. 12, no. 2/3, p. 140, 2012, doi: 10.1504/PCFD.2012.047457.

[26] R. Berger, C. Kloss, A. Kohlmeyer, and S. Pirker, “Hybrid parallelization of the LIGGGHTS open-source DEM code,” *Powder Technology*, vol. 278, pp. 234–247, Jul. 2015, doi: 10.1016/j.powtec.2015.03.019.

[27] H. Wei, Y. Zhao, J. Zhang, H. Saxén, and Y. Yu, “LIGGGHTS and EDEM application on charging system of ironmaking blast furnace,” *Advanced Powder Technology*, vol. 28, no. 10, pp. 2482–2487, Oct. 2017, doi: 10.1016/j.apt.2017.05.012.

[28] C. Kloss and C. Goniva, “LIGGGHTS - Open Source Discrete Element Simulations of Granular Materials Based on Lammps,” in *Supplemental Proceedings*, Hoboken, NJ, USA: John Wiley & Sons, Inc., 2011, pp. 781–788. doi: 10.1002/9781118062142.ch94.

[29] R. K. Soni and R. K. Dwari, “DEM numerical studies on the design and efficiency of the continuous operating triboelectric separator,” *Advanced Powder Technology*, vol. 31, no. 4, pp. 1624–1632, Apr. 2020, doi: 10.1016/j.apt.2020.02.005.

[30] A. Hager, C. Kloss, and C. Goniva, “Combining Open Source and Easy Access in the field of DEM and coupled CFD-DEM: LIGGGHTS®, CFDEM®coupling and CFDEM®workbench,” in *Computer Aided Chemical Engineering*, Elsevier, 2018, pp. 1699–1704. doi: 10.1016/B978-0-444-64235-6.50296-5.

[31] T. Leps and C. Hartzell, “High fidelity, discrete element method simulation of magnetorheological fluids using accurate particle size distributions in LIGGGHTS extended with mutual dipole method,” *Mater. Res. Express*, vol. 8, no. 8, p. 085701, Aug. 2021, doi: 10.1088/2053-1591/ac113c.

[32] C. Ramírez-Aragón, J. Ordieres-Meré, F. Alba-Elías, and A. González-Marcos, “Comparison of Cohesive Models in EDEM and LIGGGHTS for Simulating Powder Compaction,” *Materials*, vol. 11, no. 11, p. 2341, Nov. 2018, doi: 10.3390/ma11112341.

[33] A. H. Madadi Najafabadi, A. Masoumi, and S. M. Vaez Allaei, “Analysis of abrasive damage of iron ore pellets,” *Powder Technology*, vol. 331, pp. 20–27, May 2018, doi: 10.1016/j.powtec.2018.02.030.

[34] M. Jahani, A. Farzanegan, and M. Noaparast, “Investigation of screening performance of banana screens using LIGGGHTS DEM solver,” *Powder Technology*, vol. 283, pp. 32–47, Oct. 2015, doi: 10.1016/j.powtec.2015.05.016.

[35] S. M. Derakhshani, D. L. Schott, and G. Lodewijks, “Micro–macro properties of quartz sand: Experimental investigation and DEM simulation,” *Powder Technology*, vol. 269, pp. 127–138, Jan. 2015, doi: 10.1016/j.powtec.2014.08.072.

[36] C. Ramírez-Aragón, J. Ordieres-Meré, F. Alba-Elías, and A. González-Marcos, “Numerical Modeling for Simulation of Compaction of Refractory Materials for Secondary Steelmaking,” *Materials*, vol. 13, no. 1, p. 224, Jan. 2020, doi: 10.3390/ma13010224.

[37] P. Dutta, S. Mandal, and A. Kumar, “Comparative study: FPA based response surface methodology & ANOVA for the parameter optimization in process control,” *AMA_C*, vol. 73, no. 1, pp. 23–27, Mar. 2018, doi: 10.18280/ama_c.730104.

[38] A. Bensaha, F. Benkouider, Sma. Bekkouche, A. Abdellaoui, T. Chergui, and A. Benseddik, “An Experimental Study of an Evacuated Tube Solar Collector Using the Response Surface Methodology (RSM),” *MMC_B*, vol. 88, no. 2–4, pp. 106–111, Dec. 2019, doi: 10.18280/mmc_b.882-414.

[39] N. V. S. R. Yellapragada *et al.*, “Application of Taguchi – PCA/GRA Method to Optimize the Wear Behaviour of Polyester/Carbon Fibre Composites,” *RCMA*, vol. 33, no. 2, pp. 65–73, Apr. 2023, doi: 10.18280/rcma.330201.

[40] B. Rudiyanto, M. Andrianto, B. Piluharto, and M. Hijriawan, “Design-Based Response Surface Methodology in Optimizing the Dry Washing Purification Process of Biodiesel from Waste Cooking Oil,” *IJHT*, vol. 40, no. 2, pp. 561–568, Apr. 2022, doi: 10.18280/ijht.400224.

[41] A. Becze, V. L. Babalau-Fuss, C. Varaticeanu, and C. Roman, “Optimization of High-Pressure Extraction Process of Antioxidant Compounds from Feteasca regala Leaves Using Response Surface Methodology,” *Molecules*, vol. 25, no. 18, p. 4209, Sep. 2020, doi: 10.3390/molecules25184209.

[42] A. Daraee, S. M. Ghoreishi, and A. Hedayati, “Supercritical CO2 extraction of chlorogenic acid from sunflower (Helianthus annuus) seed kernels: modeling and optimization by response surface methodology,” *The Journal of Supercritical Fluids*, vol. 144, pp. 19–27, Feb. 2019, doi: 10.1016/j.supflu.2018.10.001.

[43] O. D. Mante, F. A. Agblevor, and R. McClung, “A study on catalytic pyrolysis of biomass with Y-zeolite based FCC catalyst using response surface methodology,” *Fuel*, vol. 108, pp. 451–464, Jun. 2013, doi: 10.1016/j.fuel.2012.12.027.

[44] B. Rudiyanto, M. Andrianto, B. Piluharto, and M. Hijriawan, “Design-Based Response Surface Methodology in Optimizing the Dry Washing Purification Process of Biodiesel from Waste Cooking Oil,” *IJHT*, vol. 40, no. 2, pp. 561–568, Apr. 2022, doi: 10.18280/ijht.400224.

[45] I. Taymaz, F. Akgun, and M. Benli, “Application of response surface methodology to optimize and investigate the effects of operating conditions on the performance of DMFC,” *Energy*, vol. 36, no. 2, pp. 1155–1160, Feb. 2011, doi: 10.1016/j.energy.2010.11.034.

[46] D. Pinheiro, K. R. Sunaja Devi, A. Jose, N. Rajiv Bharadwaj, and K. J. Thomas, “Effect of surface charge and other critical parameters on the adsorption of dyes on SLS coated ZnO nanoparticles and optimization using response surface methodology,” *Journal of Environmental Chemical Engineering*, vol. 8, no. 4, p. 103987, Aug. 2020, doi: 10.1016/j.jece.2020.103987.

[47] S. Simsek and S. Uslu, “Investigation of the effects of biodiesel/2-ethylhexyl nitrate (EHN) fuel blends on diesel engine performance and emissions by response surface methodology (RSM),” *Fuel*, vol. 275, p. 118005, Sep. 2020, doi: 10.1016/j.fuel.2020.118005.